ELSEVIER

Chemical Physics 190 (1995) 179–189

Chemical Physics

Fourfold clusters of rovibrational energies in H_2Te studied with an ab initio potential energy function

Per Jensen [a,*], Yan Li [b], Gerhard Hirsch [b], Robert J. Buenker [b], Timothy J. Lee [c], Igor N. Kozin [d]

[a] *Physikalisch-Chemisches Institut, Justus-Liebig-Universität Giessen, Heinrich-Buff-Ring 58, D-35392 Giessen, Germany*
[b] *FB 9-Theoretische Chemie, Bergische Universität–Gesamthochschule Wuppertal, D-42097 Wuppertal, Germany*
[c] *NASA Ames Research Center, Moffett Field, CA 94035, USA*
[d] *Applied Physics Institute, Russian Academy of Science, Uljanov Street 46, 630 600 GSP-120 Nizhnii Novgorod, Russian Federation*

Received 9 May 1994; in final form 11 July 1994

Abstract

We report here an ab initio investigation of the cluster effect (i.e., the formation of four-member groups of nearly degenerate rotation–vibration energy levels at higher J and K_a values) in the H_2Te molecule. The potential energy function has been calculated ab initio at a total of 334 molecular geometries by means of the CCSD(T) method where the (1s–4f) core electrons of the Te atom were described by an effective core potential. The values of the potential energy function obtained cover the region up to around 10 000 cm^{-1} above the equilibrium energy. On the basis of the ab initio potential, the rotation–vibration energy spectra of $H_2{}^{130}Te$ and its deuterated isotopomers have been calculated with the MORBID (Morse oscillator rigid bender internal dynamics) Hamiltonian and computer program. In particular, we have calculated the rotational energy manifolds for $J \leqslant 40$ in the vibrational ground state, the ν_2 state, the "first triad" (the $\nu_1/\nu_3/2\,\nu_2$ interacting vibrational states), and the "second triad" (the $(\nu_1+\nu_2)/(\nu_2+\nu_3)/3\,\nu_2$ states) of $H_2{}^{130}Te$. We have also investigated the cluster formation in the vibrational ground state of $H_2{}^{130}Te$ by first fitting the rotational data available from experiment with a modified Watson-type effective Hamiltonian and then using the optimized ground state constants to extrapolate the rotational structure to higher J values. Both the ab initio calculation and the prediction with the effective Hamiltonian show that the cluster formation in H_2Te is very similar to that in H_2Se and H_2S, which we have studied previously. However, contrary to semiclassical predictions, we do not determine any significant displacement of the clusters towards lower J values relative to H_2Se. Hence the experimental observation of the cluster states in H_2Te will be at least as difficult as in H_2Se.

1. Introduction

In recent papers [1–3] we have reported theoretical studies of the cluster effect (i.e., the formation of nearly degenerate, four-member groups of rotation–vibration energy levels at higher J and K_a values) in the H_2Se [1,2] and H_2S [3] molecules. For each of these molecules we have used the MORBID (Morse oscillator rigid bender internal dynamics) approach [4–6], first to optimize the potential energy surface on the basis of the available experimental data, and then to calculate the cluster structure for $J \leqslant 40$ in the lower vibrational states. Further, in a short note [7] we have discussed the group theoretical description of the cluster states in terms of permutation-inversion symmetry [8,9].

* Corresponding author.

SSDI 0301-0104(94)00262-2

The cluster effect has been experimentally verified for the vibrational ground state of H_2Se [10–12]. The range of J and K_a values accessible in the experiments was barely sufficient to establish unambiguously the existence of the clusters. Our calculations show, however, that in H_2Se, the clusters are found at lower J values than in H_2S, in agreement with semiclassical estimations [13–17]. The semiclassical estimations also indicate that in H_2Te, clusters should appear at J values even lower than those found for H_2Se, which would make them amenable to experimental observation.

The purpose of the present work is to investigate whether the H_2Te molecule would be a suitable candidate for further experimental verification of the cluster effect. For the molecules H_2Se and H_2S we investigated the cluster phenomenon by first optimizing a potential energy surface to reproduce the available experimental data and then extrapolating these data to $J=40$. Some experimental work has been carried out for H_2Te [18–24], mostly by Edwards and co-workers. In the electronic ground state of H_2Te, the vibrational ground state [24], the ν_2 state [19,23], the interacting states $\nu_1+\nu_2$ and $\nu_2+\nu_3$ [21], and the interacting states $2\nu_1$ and $\nu_1+\nu_3$ [23] have been spectroscopically characterized together with the vibrational ground state and the $2\nu_1$ state of HDTe [22]. In a very early, low-resolution study Rossmann and Straley [18] found that the ν_1 and ν_3 bands of H_2Te extend from 1800 to 2200 cm^{-1}. The amount of experimental information available for H_2Te is not sufficient for an optimization of the potential energy surface. Consequently, we have chosen to study the cluster formation in H_2Te on the basis of an ab initio potential energy surface calculated with the CCSD(T) method. With this surface as input, we have used the MORBID program to calculate the rotation–vibration energy spectrum of $H_2{}^{130}Te$ and its isotopomers for $J \leqslant 40$. These calculations reproduce well the experimental data described above. However, the cluster structures obtained for the vibrational ground state and the fundamental vibrational levels of H_2Te are found to be extremely similar to those determined previously for H_2Se. In particular, we do not determine any significant displacement of the clusters towards lower J values relative to H_2Se. Hence the experimental observation of the cluster states in H_2Te will be at least as difficult as in H_2Se.

2. The ab initio calculation

The potential energy surface employed in the present study was calculated using the CCSD(T) method [25], using the TITAN [1] coupled-cluster program. The (1s–4f) core electrons of the Te atom were described by an effective core potential [26]. An uncontracted (3s3p) basis [26] augmented with two sets of d orbitals was used to describe the Te valence electrons [26]. The orbital exponents for the two sets of d orbitals were 0.440 a_0^{-2} and 0.134 a_0^{-2}, respectively. A contracted [3s] basis augmented with two sets of p orbitals was chosen for the H atom [27]. The electronic energy has been calculated at a total of 334 molecular geometries, covering H–Te bond distances in the range from 2.55 to 3.95 a_0 and H–Te–H bond angles in the range from 70° to 110°. This allowed us to characterize the potential energy surface up to around 10 000 cm^{-1} above the equilibrium energy.

3. The analytical form of the potential energy function

The analytical representation of the potential energy function used in the present work is given as (see Refs. [4–6])

$$V(\Delta r_1, \Delta r_3, \bar{\rho}) = V_0(\bar{\rho}) + \sum_j F_j(\bar{\rho}) y_j + \sum_{j \leqslant k} F_{jk}(\bar{\rho}) y_j y_k + \sum_{j \leqslant k \leqslant m} F_{jkm}(\bar{\rho}) y_j y_k y_m + \sum_{j \leqslant k \leqslant m \leqslant n} F_{jkmn}(\bar{\rho}) y_j y_k y_m y_n , \quad (1)$$

where all of the indices j, k, m, and n assume the values 1 or 3. The quantity y_j in Eq. (1) is given by

$$y_j = 1 - \exp(-a_j \Delta r_j) , \quad (2)$$

where the a_j are molecular constants and $\Delta r_j = r_j - r_j^e$, $j=1$ or 3, is defined as a displacement from the equilibrium value r_j^e of the distance r_j between the "outer" nucleus $j=1$ or 3 and the "center" nucleus 2. The quantity $\bar{\rho}$ is the instantaneous value of the bond angle supplement (see Fig. 1 of Ref. [4]). The $F_{jkm\ldots}$ expan-

[1] TITAN is a set of electronic structure programs written by T.J. Lee, A.P. Rendell and J.E. Rice.

Table 1
Ab initio potential energy parameters for H_2Te

ρ_e (deg)	89.6605(178) [a]		
r_1^e (Å)	1.661640(60)		
a_1 (Å^{-1})	1.4741(16)		
$f_0^{(2)}$ (cm^{-1})	15999.3(727)	$f_1^{(1)}$ (cm^{-1})	−1362.0(245)
$f_0^{(3)}$ (cm^{-1})	1107(123)	$f_1^{(2)}$ (cm^{-1})	−4665(238)
$f_0^{(4)}$ (cm^{-1})	6554(619)	$f_1^{(3)}$ (cm^{-1})	−1070(313)
$f_{11}^{(0)}$ (cm^{-1})	31371.7(607)	$f_1^{(4)}$ (cm^{-1})	−5681(1764)
$f_{11}^{(1)}$ (cm^{-1})	139.2(501)	$f_{13}^{(0)}$ (cm^{-1})	−313.5(148)
$f_{11}^{(2)}$ (cm^{-1})	−4990(245)	$f_{13}^{(1)}$ (cm^{-1})	3111(198)
$f_{111}^{(2)}$ (cm^{-1})	−1886(731)	$f_{13}^{(2)}$ (cm^{-1})	3123(358)
$f_{113}^{(0)}$ (cm^{-1})	−261.4(265)	$f_{13}^{(3)}$ (cm^{-1})	3670(1586)
$f_{113}^{(2)}$ (cm^{-1})	1475(634)	$f_{1111}^{(0)}$ (cm^{-1})	871.2(449)
$f_{1133}^{(0)}$ (cm^{-1})	277.0(652)	$f_{1113}^{(1)}$ (cm^{-1})	−1081(297)
$f_{1133}^{(1)}$ (cm^{-1})	−1072(448)		

[a] Quantities in parentheses are standard errors in units of the last digit given.

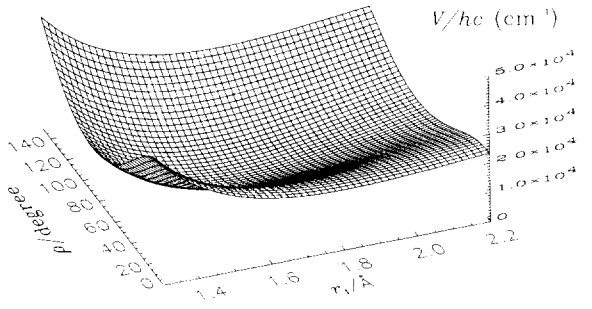

Fig. 1. A section of the fitted potential energy surface. V is shown as a function of the angle $\rho = \pi - \alpha$, where α is the bond angle, and the bond distance r_1. The bond distance r_3 is held fixed at its equilibrium value.

Table 2
Conventional force constants for H_2Te

f_{rr} (aJ Å^{-2})	2.708	f_{rrrr} (aJ Å^{-4})	43.153
$f_{\alpha\alpha}$ (aJ)	0.636	$f_{\alpha\alpha\alpha\alpha}$ (aJ)	0.587
$f_{rr'}$ (aJ Å^{-2})	−0.014	$f_{rrrr'}$ (aJ Å^{-4})	0.118
$f_{r\alpha}$ (aJ Å^{-1})	0.040	$f_{rrr'r'}$ (aJ Å^{-4})	0.173
f_{rrr} (aJ Å^{-3})	−11.976	$f_{rrr\alpha}$ (aJ Å^{-3})	0.140
$f_{\alpha\alpha\alpha}$ (aJ)	−0.143	$f_{rrr'\alpha}$ (aJ Å^{-3})	0.217
$f_{rrr'}$ (aJ Å^{-3})	−0.133	$f_{rr\alpha\alpha}$ (aJ Å^{-2})	−0.458
$f_{rr\alpha}$ (aJ Å^{-2})	−0.071	$f_{rr'\alpha\alpha}$ (aJ Å^{-2})	0.270
$f_{rr'\alpha}$ (aJ Å^{-2})	−0.147	$f_{r\alpha\alpha\alpha}$ (aJ Å^{-1})	0.153
$f_{r\alpha\alpha}$ (aJ Å^{-1})	−0.273		

sion coefficients of Eq. (1) are functions of $\bar{\rho}$ and defined as

$$F_j(\bar{\rho}) = \sum_{i=1}^{4} f_j^{(i)} (\cos\rho_e - \cos\bar{\rho})^i , \qquad (3)$$

and

$$F_{jk\ldots}(\bar{\rho}) = f_{jk\ldots}^{(0)} + \sum_{i=1}^{N} f_{jk\ldots}^{(i)} (\cos\rho_e - \cos\bar{\rho})^i , \qquad (4)$$

where ρ_e is the equilibrium value of $\bar{\rho}$ and the $f_{jk\ldots}^{(i)}$ are expansion coefficients. The function $F_{jk}(\bar{\rho})$ has $N=3$, $F_{jkl}(\bar{\rho})$ has $N=2$, and $F_{jklm}(\bar{\rho})$ has $N=1$. The function $V_0(\bar{\rho})$ is the potential energy for the molecule bending with bond lengths fixed at their equilibrium values, and here we parameterize it as

$$V_0(\bar{\rho}) = \sum_{i=2}^{8} f_0^{(i)} (\cos\rho_e - \cos\bar{\rho})^i . \qquad (5)$$

where the $f_0^{(i)}$ are expansion coefficients.

We have obtained values for the parameters of the analytical function in Eqs. (1)–(5) by fitting it on the basis of the 334 ab initio points calculated for H_2Te. By varying 25 parameters we achieved a fit with a standard deviation of 13.8 cm^{-1}. The values of the fitted parameters are given in Table 1, and Fig. 1 shows a graphical representation of a section of the fitted surface.

In Table 2 we give values for the standard "force constants" of H_2Te. These constants are defined as the first to fourth derivatives at equilibrium ($\Delta r_1 = \Delta r_3 = 0$, $\bar{\rho} = \rho_e$) of the potential energy function given by Eqs. (1)–(5) with the parameters of Table 1, e.g.,

$$f_{rr} = \left(\frac{\partial^2 V}{\partial \Delta r_1^2}\right)_e , \tag{6}$$

$$f_{r\alpha} = \left(\frac{\partial^2 V}{\partial \Delta r_1 \partial \alpha}\right)_e , \tag{7}$$

etc., $\alpha = \pi - \bar{\rho}$ being the bond angle.

4. The calculation of the rotation–vibration energies

The rotation–vibration calculations reported in the present work have been carried out with the MORBID Hamiltonian and computer program. This theoretical approach to calculate the rotation–vibration energies of a triatomic molecule has been extensively described elsewhere [4–6] and we refer the reader to these publications for details. We note that in the MORBID approach, we express the kinetic energy operator as a fourth order Taylor expansion in the stretching functions y_1 and y_3. Because of this approximation, a MORBID calculation requires significantly less CPU time than calculations with other methods employing an exact kinetic energy operator [28–31].

We have carried out MORBID calculations with the following basis sets:

I. The $J=0$ and 1 energies of $H_2{}^{130}Te$ and $D_2{}^{130}Te$ were calculated with a basis set (see Ref. [4]) in which the stretching problem was prediagonalized with Morse oscillator functions $|n_1 n_3\rangle$ having $n_1 + n_3 \leqslant N_{\text{Stretch}} = 16$. In constructing the final rotation–vibration matrices we used the $N_{\text{Bend}} = 13$ lowest bending basis functions, the $N_A = 25$ lowest stretching basis functions of A_1 symmetry and the $N_B = 20$ lowest stretching basis functions of B_2 symmetry.

II. The $J=0$ and 1 energies of $HD^{130}Te$ were calculated with a basis set having $N_{\text{Stretch}} = 16$, $N_{\text{Bend}} = 13$, and $N_A = 55$.

III. The $J \leqslant 40$ energies of $H_2{}^{130}Te$ in selected vibrational states were calculated with a basis set having $N_{\text{Stretch}} = 7$, $N_{\text{Bend}} = 8$, and $(N_A, N_B) = (6, 4)$.

The results of calculations I and II are given in Tables 3–5. Table 3 gives the calculated vibrational energies for $H_2{}^{130}Te$ up to the $3\nu_3$ state at 6135 cm^{-1} together with values of the rotational constants A, B, and C estimated from the $J=0$ and 1 energies by means of the rigid rotor equations (see, for example, ch. 8 of Ref. [8])

$$\begin{aligned} E(1_{01}) - E(0_{00}) &= B + C , \\ E(1_{11}) - E(0_{00}) &= A + C , \\ E(1_{10}) - E(0_{00}) &= A + B , \end{aligned} \tag{8}$$

where the energies are labeled by $J_{K_a K_c}$. Tables 4 and 5 give analogous results for $D_2{}^{130}Te$ and $HD^{130}Te$, respectively.

The results of calculation III are presented graphically in Figs. 2–5. Fig. 2 shows the rotational energy level structure in the vibrational ground state of $H_2{}^{130}Te$. The term values are plotted relative to the highest term value for each J multiplet. The term values computed by the MORBID program (using the parameters from Table 1) are given as horizontal lines. The circles represent term values calculated with a modified Watson-type effective Hamiltonian obtained from the effective Hamiltonian described in Refs. [10,12] by retaining terms with powers of angular momentum components up to (and including) eight:

$$\begin{aligned} \hat{H} = {} & \tfrac{1}{2}(B+C)\hat{J}^2 + [A - \tfrac{1}{2}(B+C)]\hat{J}_z^2 - D_J \hat{J}^4 \\ & - D_{JK}\hat{J}^2\hat{J}_z^2 - D_K \hat{J}_z^4 + H_J \hat{J}^6 + H_{JK}\hat{J}^4\hat{J}_z^2 \\ & + H_{KJ}\hat{J}^2\hat{J}_z^4 + H_K \hat{J}_z^6 + c_{40}(\hat{J}^2 - \hat{J}_z^2)^4 \\ & + c_{31}(\hat{J}^2 - \hat{J}_z^2)^3\hat{J}_z^2 + c_{22}(\hat{J}^2 - \hat{J}_z^2)^2\hat{J}_z^4 \\ & + c_{13}(\hat{J}^2 - \hat{J}_z^2)\hat{J}_z^6 + c_{04}\hat{J}_z^8 \\ & + \tfrac{1}{2}[\{\tfrac{1}{4}(B-C) - d_J\hat{J}^2 - d_K\hat{J}_z^2 + h_J\hat{J}^4 + h_{JK}\hat{J}^2\hat{J}_z^2 \\ & + h_K\hat{J}_z^4 + b_{30}(\hat{J}^2 - \hat{J}_z^2)^3 + b_{21}(\hat{J}^2 - \hat{J}_z^2)^2\hat{J}_z^2 \\ & + b_{12}(\hat{J}^2 - \hat{J}_z^2)\hat{J}_z^4 + b_{03}\hat{J}_z^6\}, \{\hat{J}_+^2 + \hat{J}_-^2\}]_+ , \end{aligned} \tag{9}$$

where $\hat{J}_x$, $\hat{J}_y$ and $\hat{J}_z$ are the components of the total angular momentum along the molecule-fixed axes, $\hat{J}^2 = \hat{J}_x^2 + \hat{J}_y^2 + \hat{J}_z^2$, $\hat{J}_\pm = \hat{J}_x \pm i\hat{J}_y$, and the plus commutator of two operators $\hat{A}$ and $\hat{B}$ is $[\hat{A}, \hat{B}]_+ = \hat{A}\hat{B} + \hat{B}\hat{A}$. The parameters used in calculating the term values displayed in Fig. 2 were determined by fitting 29 rotational transitions reported in Ref. [24] and 186 ground state combination differences computed from the infrared data of Ref. [21]. In this fit, 17 parameters were varied. Their optimized values are given in Table 6. Parameters, whose values are not given in the table, were found to have absolute values smaller than their standard errors and were constrained to zero. The root-mean-

Table 3
Predicted rotation–vibration parameters for $H_2{}^{130}Te$ (in cm^{-1})

(v_1, v_2, v_3) [a]	$(nm^{\pm} v_2)$ [b]	E_{vib}	A	B	C
(0, 0, 0)	$(00^{+}\ 0)$	0.0	6.1860	6.0182	3.0020
(0, 1, 0)	$(00^{+}\ 1)$	866.85	6.3559	6.1488	2.9721
(0, 2, 0)	$(00^{+}\ 2)$	1731.01	6.5343	6.2869	2.9417
(1, 0, 0)	$(10^{+}\ 0)$	2061.27	6.1093	5.9381	2.9614
(0, 0, 1)	$(10^{-}\ 0)$	2070.42	6.0846	5.9630	2.9715
(0, 3, 0)	$(00^{+}\ 3)$	2591.35	6.7230	6.4337	2.9109
(1, 1, 0)	$(10^{+}\ 1)$	2914.47	6.2770	6.0674	2.9297
(0, 1, 1)	$(10^{-}\ 1)$	2921.13	6.2493	6.0957	2.9434
(0, 4, 0)	$(00^{+}\ 4)$	3446.82	6.9243	6.5903	2.8800
(1, 2, 0)	$(10^{+}\ 2)$	3764.66	6.4519	6.2056	2.8954
(0, 2, 1)	$(10^{-}\ 2)$	3768.96	6.4208	6.2376	2.9168
(2, 0, 0)	$(20^{+}\ 0)$	4060.10	6.0032	5.8858	2.9008
(1, 0, 1)	$(20^{-}\ 0)$	4061.00	5.9967	5.8925	2.9565
(0, 0, 2)	$(11^{+}\ 0)$	4132.05	6.0048	5.8863	2.9336
(0, 5, 0)	$(00^{+}\ 5)$	4296.44	7.1404	6.7582	2.8489
(1, 3, 0)	$(10^{+}\ 3)$	4610.78	6.6305	6.3591	2.8511
(0, 3, 1)	$(10^{-}\ 3)$	4612.82	6.5955	6.3955	2.8996
(2, 1, 0)	$(20^{+}\ 1)$	4897.45	6.1325	6.0504	2.8232
(1, 1, 1)	$(20^{-}\ 1)$	4897.76	6.1269	6.0562	2.9744
(0, 1, 2)	$(11^{+}\ 1)$	4968.67	6.1709	6.0142	2.9037
(0, 6, 0)	$(00^{+}\ 6)$	5139.24	7.3742	6.9392	2.8179
(0, 4, 1)	$(10^{-}\ 4)$	5451.66	6.9154	6.4307	2.8247
(1, 4, 0)	$(10^{+}\ 4)$	5451.83	6.9547	6.3895	2.8638
(1, 2, 1)	$(20^{-}\ 2)$	5731.36	6.4265	6.0666	2.8623
(2, 2, 0)	$(20^{+}\ 2)$	5731.45	6.4309	6.0620	2.8744
(0, 2, 2)	$(11^{+}\ 2)$	5802.29	6.3458	6.1495	2.8733
(0, 7, 0)	$(00^{+}\ 7)$	5974.31	7.6289	7.1348	2.7870
(2, 0, 1)	$(30^{-}\ 0)$	5985.28	6.1017	5.6274	2.9103
(3, 0, 0)	$(30^{+}\ 0)$	5985.34	6.1020	5.6270	2.8715
(1, 0, 2)	$(21^{+}\ 0)$	6117.02	5.9420	5.7904	2.8877
(0, 0, 3)	$(21^{-}\ 0)$	6134.66	5.8965	5.8370	2.9045

[a] Normal mode labels.
[b] Local mode labels.

square deviations obtained were 0.094 MHz for the rotational lines and 0.0064 cm^{-1} for the combination differences. These values are in keeping with the experimental accuracies of the fitted data and with the fact that the infrared data are combination differences. The accuracy of the infrared transition wavenumbers, which were measured 20 years ago, is probably around 0.005 cm^{-1}. The input data involved rotational states with $J \leqslant 13$, $K_a \leqslant 8$, and $K_c \leqslant 12$. The highest available energy level of the type $J_{K_aK_c} = J_{J0}$ was the 7_{70} level. The matrix elements of the Watson-type Hamiltonian are given as power series expansions in the rotational quantum numbers, and as J increases, these expansions eventually become divergent. Consequently, with this Hamiltonian it is not feasible to predict the energy structure to arbitrarily high J values. We have used it to predict the rotational energy levels of the vibrational ground state of $H_2{}^{130}Te$ with $J \leqslant 20$. For this range of J values, no convergence problems occur. The filled circles in Fig. 2 represent term values for states involved in the rotational transitions or in the combination differences which were used as input for the fitting with the Hamiltonian of Eq. (9), whereas the empty circles represent term values predicted with this Hamiltonian.

Figs. 3–5 are term value diagrams for the ν_2 vibrational state, the $\nu_1/\nu_3/2\nu_2$ interacting vibrational states, and the $(\nu_1+\nu_2)/(\nu_2+\nu_3)/3\nu_2$ interacting vibrational states, of $H_2{}^{130}Te$, respectively. In these three figures, the term values are plotted relative to the

Table 4
Predicted rotation–vibration parameters for $D_2{}^{130}Te$ (in cm^{-1})

(v_1, v_2, v_3) [a]	$(nm^{\pm} v_2)$ [b]	E_{vib}	A	B	C
(0, 0, 0)	$(00^{+}\ 0)$	0.0	3.1429	3.0120	1.5208
(0, 1, 0)	$(00^{+}\ 1)$	619.12	3.2033	3.0579	1.5101
(0, 2, 0)	$(00^{+}\ 2)$	1237.18	3.2657	3.1057	1.4993
(1, 0, 0)	$(10^{+}\ 0)$	1479.38	3.1164	2.9827	1.5067
(0, 0, 1)	$(10^{-}\ 0)$	1486.46	3.1065	2.9925	1.5097
(0, 3, 0)	$(00^{+}\ 3)$	1853.74	3.3305	3.1554	1.4884
(1, 1, 0)	$(10^{+}\ 1)$	2091.69	3.1765	3.0282	1.4958
(0, 1, 1)	$(10^{-}\ 1)$	2097.50	3.1657	3.0389	1.4992
(0, 4, 0)	$(00^{+}\ 4)$	2468.42	3.3978	3.2073	1.4774
(1, 2, 0)	$(10^{+}\ 2)$	2702.82	3.2385	3.0755	1.4847
(0, 2, 1)	$(10^{-}\ 2)$	2707.41	3.2268	3.0871	1.4887
(2, 0, 0)	$(20^{+}\ 0)$	2929.01	3.0828	2.9601	1.4919
(1, 0, 1)	$(20^{-}\ 0)$	2930.27	3.0790	2.9638	1.4976
(0, 0, 2)	$(11^{+}\ 0)$	2966.77	3.0766	2.9666	1.4967
(0, 5, 0)	$(00^{+}\ 5)$	3080.84	3.4682	3.2616	1.4664
(1, 3, 0)	$(10^{+}\ 3)$	3312.35	3.3026	3.1250	1.4732
(0, 3, 1)	$(10^{-}\ 3)$	3315.78	3.2901	3.1375	1.4784
(2, 1, 0)	$(20^{+}\ 1)$	3533.59	3.1404	3.0072	1.4797
(1, 1, 1)	$(20^{-}\ 1)$	3534.39	3.1369	3.0106	1.4886
(0, 1, 2)	$(11^{+}\ 1)$	3570.61	3.1362	3.0119	1.4860
(0, 6, 0)	$(00^{+}\ 6)$	3690.62	3.5420	3.3184	1.4553
(1, 4, 0)	$(10^{+}\ 4)$	3919.91	3.3690	3.1769	1.4609
(0, 4, 1)	$(10^{-}\ 4)$	3922.19	3.3554	3.1906	1.4688
(2, 2, 0)	$(20^{+}\ 2)$	4136.82	3.1974	3.0586	1.4646
(1, 2, 1)	$(20^{-}\ 2)$	4137.26	3.1944	3.0617	1.4822
(0, 2, 2)	$(11^{+}\ 2)$	4173.28	3.1977	3.0588	1.4752
(0, 7, 0)	$(00^{+}\ 7)$	4297.42	3.6197	3.3782	1.4442
(3, 0, 0)	$(30^{+}\ 0)$	4341.59	3.0945	2.8917	1.4938
(2, 0, 1)	$(30^{-}\ 0)$	4341.64	3.0940	2.8921	1.4695
(1, 0, 2)	$(21^{+}\ 0)$	4406.07	3.0566	2.9306	1.4807
(0, 0, 3)	$(21^{-}\ 0)$	4419.78	3.0380	2.9491	1.4860

[a] Normal mode labels.
[b] Local mode labels.

highest term value in each J multiplet *of the vibrational ground state.*

5. Discussion

In Table 7 we compare vibrational energy values and the rotational constants calculated ab initio in the present work with the available experimental data [19–24]. We see that our purely theoretical calculation reproduces the observed quantities very satisfactorily. The deviations are only around 1% in the worst cases.

From the ab initio calculation described in Section 2, we obtain the equilibrium bond angle of H_2Te as $\alpha_e = \pi - \rho_e = 90.340°$ and the equilibrium bond length $r_1^e = 1.66164$ Å. These values can be compared with the experimentally derived values of Moncur et al. [23], $\alpha_e = 90.25°$ and $r_1^e = 1.658$ Å. Again, the agreement is very good. The deviations are only 0.1% for α_e and 0.2% for r_1^e. In a fairly recent ab initio study of H_2Te, in which the potential energy surface was obtained using the relativistic complete active space multiconfiguration self-consistent field (CASSCF) method followed by full second-order configuration interaction (SOCI) and relativistic configuration interaction (RCI) calculations involving spin–orbit coupling, Sumathi and Balasubramanian [32] determined $\alpha_e = 91.2°$ and $r_1^e = 1.668$ Å.

In view of the good agreement between experiment and theory obtained in the present work, we conclude

Table 5
Predicted rotation–vibration parameters for $HD^{130}Te$ (in cm^{-1})

(v_1, v_2, v_3)	E_{vib}	A	B	C
(0, 0, 0)	0.0	6.1005	3.0741	2.0191
(0, 1, 0)	753.61	6.2432	3.1240	2.0030
(0, 0, 1)	1482.55	6.0998	3.0196	1.9972
(0, 2, 0)	1505.30	6.3915	3.1757	1.9866
(1, 0, 0)	2066.04	5.9460	3.0729	2.0027
(0, 1, 1)	2228.14	6.2450	3.0696	1.9810
(0, 3, 0)	2254.40	6.5454	3.2296	1.9701
(1, 1, 0)	2805.08	6.0865	3.1217	1.9866
(0, 0, 2)	2929.58	6.0984	2.9646	1.9749
(0, 2, 1)	2971.53	6.3990	3.1221	1.9646
(0, 4, 0)	3000.30	6.7048	3.2856	1.9534
(1, 2, 0)	3541.83	6.2293	3.1681	1.9704
(1, 0, 1)	3547.91	5.9494	3.0231	1.9808
(0, 1, 2)	3667.19	6.2429	3.0143	1.9588
(0, 3, 1)	3711.95	6.5638	3.1779	1.9480
(0, 5, 0)	3742.48	6.8687	3.3436	1.9366
(2, 0, 0)	4061.63	5.7895	3.0716	1.9857
(1, 3, 0)	4274.89	6.3296	3.1843	1.9572
(1, 1, 1)	4279.86	6.1436	3.1096	1.9612
(0, 0, 3)	4341.02	6.0971	2.9092	1.9523
(0, 2, 2)	4402.40	6.3968	3.0665	1.9425
(0, 4, 1)	4448.70	6.7421	3.2378	1.9312
(0, 6, 0)	4480.50	7.0354	3.4033	1.9198
(2, 1, 0)	4785.97	5.9273	3.1194	1.9696
(1, 0, 2)	4993.52	5.9537	2.9647	1.9586
(1, 4, 0)	5003.37	6.4304	3.2016	1.9435
(1, 2, 1)	5010.71	6.3482	3.1968	1.9419
(0, 1, 3)	5070.85	6.2385	2.9588	1.9365
(0, 3, 2)	5134.44	6.5626	3.1218	1.9260
(0, 5, 1)	5181.06	6.9366	3.3032	1.9142
(0, 7, 0)	5214.01	7.2023	3.4639	1.9029
(2, 2, 0)	5507.92	6.0720	3.1687	1.9531
(2, 0, 1)	5542.83	5.7886	3.0175	1.9642
(1, 1, 2)	5714.95	6.1031	2.9693	1.9387
(0, 0, 4)	5717.51	6.1062	2.9011	1.9327
(1, 5, 0)	5727.73	6.5808	3.2471	1.9273
(1, 3, 1)	5738.85	6.5103	3.2588	1.9247
(0, 2, 3)	5798.07	6.3898	3.0107	1.9203
(0, 4, 2)	5862.54	6.7441	3.1816	1.9093
(0, 6, 1)	5908.37	7.1496	3.3752	1.8970
(0, 8, 0)	5942.78	7.3660	3.5242	1.8860
(3, 0, 0)	5986.60	5.6312	3.0704	1.9679

that both aspects of the theoretical approach, i.e., both the ab initio computation of the potential energy surface and the MORBID calculation of the rotation–vibration energies, provide realistic descriptions of nature.

The calculated rotational structures for the vibrational ground state and the fundamental vibrational states of $H_2{}^{130}Te$ (Figs. 2–4) are qualitatively very similar to those given for H_2Se and H_2S in Refs. [1–3]. In the vibrational ground state (Fig. 2) and in the ν_2 state (Fig. 3) we observe the formation of type I fourfold clusters [2,3] in that around $J=25$, the two highest doublets of the J manifold merge to form a group of four near-degenerate levels. In the ν_1/ν_3 interacting states (Fig. 4), we observe the formation of type II fourfold clusters [2,3,17] in that around $J=17$, the highest doublet in the ν_3 J manifold coalesces with the highest doublet in the ν_1 J manifold to form a fourfold cluster. We also observe the avoided crossing between the "top" fourfold cluster (the cluster at highest

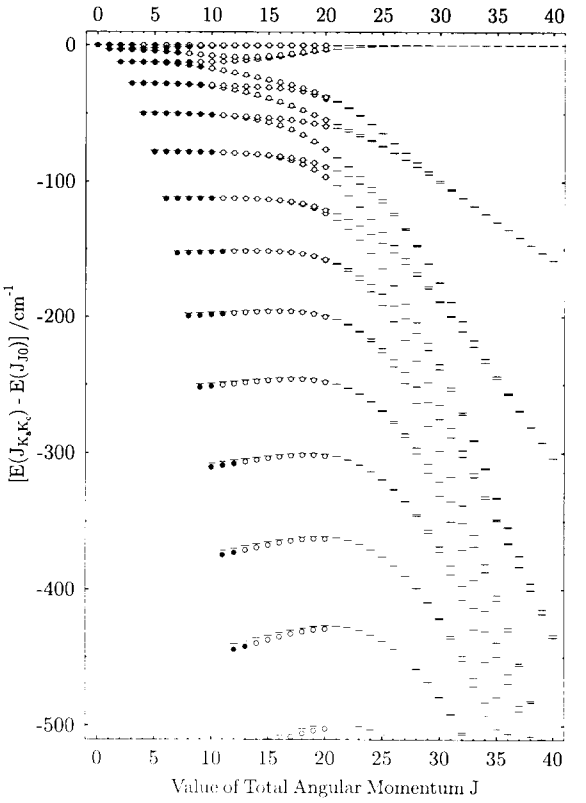

Fig. 2. The rotational energy level structure in the vibrational ground state of $H_2{}^{130}Te$. Term values are plotted relative to the highest term value for each J multiplet. The term values calculated by the MORBID program (using the parameters from Table 1) are given as horizontal lines. The circles represent term values obtained with the Watson-type effective Hamiltonian of Eq. (9) fitted to the available experimental data (see the text). Filled circles show term values for states involved in the rotational transitions or in the combination differences which were used as input for the fitting with the Watson-type Hamiltonian, whereas the empty circles represent term values predicted with this Hamiltonian.

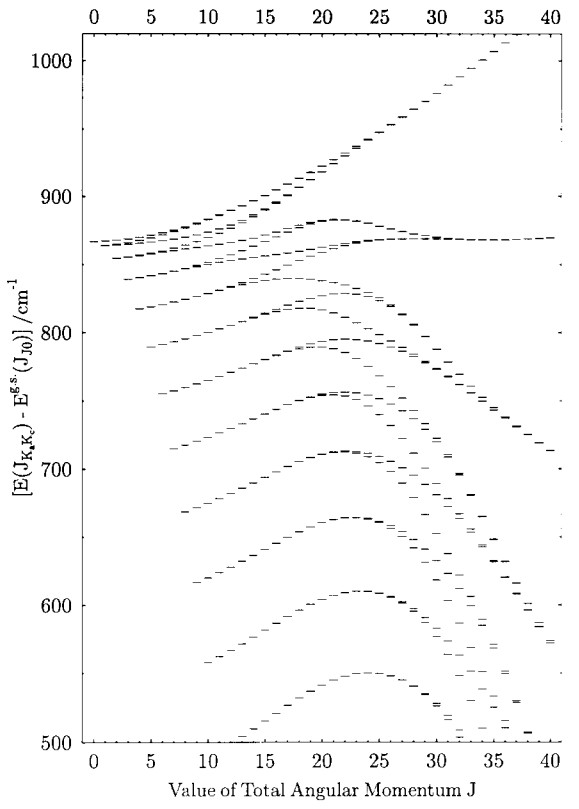

Fig. 3. The calculated rotational energy level structure in the ν_2 vibrational state of $H_2{}^{130}Te$. Term values are plotted relative to the highest term value for each J multiplet in the vibrational ground state.

energy) in the ν_1/ν_3 state and the top cluster in the $2\nu_2$ state discussed previously for H_2Se and H_2S [2,3]. In $H_2{}^{130}Te$, this avoided crossing takes place around $J=38$.

Comparison of Figs. 4 and 5 shows that also in the "second triad" (the $(\nu_1+\nu_2)/(\nu_2+\nu_3)/3\nu_2$ interacting vibrational states; Fig. 5) type II clusters are formed. As expected, the energy pattern of the second triad is similar in structure to that of the "first triad" (the $\nu_1/\nu_3/2\nu_2$ interacting vibrational states; Fig. 4). However, Fig. 5 shows more dramatic avoided crossings than does Fig. 4. Hence it would appear that in the second triad, the interaction between on one hand the $(\nu_1+\nu_2)/(\nu_2+\nu_3)$ states and on the other hand the $3\nu_2$ state is stronger than the analogous interactions between the ν_1/ν_3 states and the $2\nu_2$ state in the first triad.

Fig. 2 presents two entirely independent predictions of the cluster structure in the vibrational ground state of $H_2{}^{130}Te$. The horizontal lines in the figure give the results of a MORBID calculation using the ab initio potential energy surface obtained in the present work, whereas the circles represent term values calculated completely independently by means of the Watson-type effective Hamiltonian of Eq. (9), using as input the parameter values given in Table 6. It is seen that the two predictions agree well, especially for the top cluster. Consequently, we have conclusive evidence that for J as high as 20, the two doublets at highest energy in the vibrational ground state are separated by several cm^{-1}. The ab initio calculation predicts this separation to be 3.8 cm^{-1}, whereas the effective Watson-type Hamiltonian yields 3.1 cm^{-1}. According to the ab initio calculation, the difference decreases to 0.6 cm^{-1} at $J=25$ and to 0.04 cm^{-1} at $J=30$. For $H_2{}^{80}Se$, the MORBID calculation from Ref. [2] gives the cor-

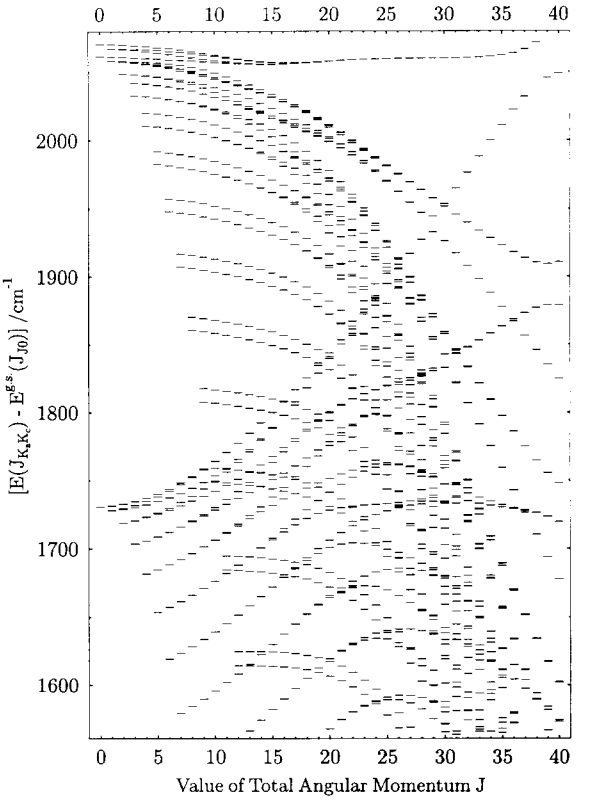

Fig. 4. An overview of the calculated rotation–vibration term values for $H_2{}^{130}Te$ in the $\nu_1/\nu_3/2\nu_2$ region. The term values are plotted relative to the highest energy for each J multiplet in the vibrational ground state. The three states present for $J=0$ are the ν_3 (at 2070 cm^{-1}), ν_1 (at 2061 cm^{-1}), and $2\nu_2$ (at 1731 cm^{-1}) levels.

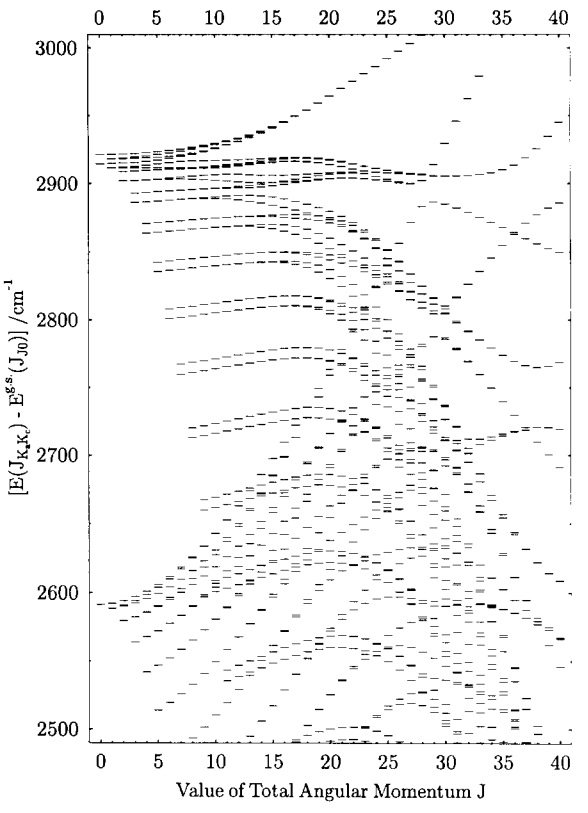

Fig. 5. An overview of the calculated rotation–vibration term values for $H_2{}^{130}Te$ in the $(\nu_1+\nu_2)/(\nu_2+\nu_3)/3\nu_2$ region. The term values are plotted relative to the highest energy for each J multiplet in the vibrational ground state. The three states present for $J=0$ are the $\nu_2+\nu_3$ (at 2921 cm^{-1}), $\nu_1+\nu_2$ (at 2914 cm^{-1}), and $3\nu_2$ (at 2591 cm^{-1}) levels.

responding splittings as 9.8 cm^{-1} at $J=20$, 1.6 cm^{-1} at $J=25$, and 0.1 cm^{-1} at $J=30$. Obviously the cluster formation in $H_2{}^{130}Te$ takes place at lower J values than in $H_2{}^{80}Se$, but the shift is not dramatic. For both molecules, the "size" of a cluster (defined as the energy difference between the cluster component at highest energy and that at lowest energy) at $J=30$ is still larger than the resolution of a high-resolution infrared spectroscopic experiment.

For the type II clusters in the ν_1/ν_3 interacting states, the situation is similar to that described above for the vibrational ground state, at least for $J\leqslant 20$. In this J range, the sizes of the $H_2{}^{130}Te$ clusters are 2–3 times smaller than the sizes of the $H_2{}^{80}Se$ clusters. For J above 20 the cluster formation in $H_2{}^{130}Te$ accelerates relative to $H_2{}^{80}Se$. According to the MORBID calculations of the present work and of Ref. [2], the cluster sizes at $J=25$ are 0.007 and 0.068 cm^{-1} for $H_2{}^{130}Te$ and $H_2{}^{80}Se$, respectively, and the corresponding splittings for $J=30$ are 0.001 and 0.009 cm^{-1}. It seems unlikely, however, that it will be possible to follow experimentally the formation of type II clusters to these high J values since in a recent experimental study of the ν_1/ν_3 state of $H_2{}^{80}Se$ [33] the high-energy part of the rotational structure could only be followed to $J=13$.

In Refs. [1–3] we have discussed the cluster formation in H_2S, H_2Se, and H_2Te in terms of the so-called critical J-value J_{cr} at which semiclassical theory expects the deviation of the rotational structure from the customary rigid-rotor picture to become apparent in the vibrational ground state (see Eq. (4) of Ref. [10]). The critical J-value is given by

$$J_{cr}=\frac{\omega}{4A}\sqrt{\frac{A-B}{C}}, \tag{10}$$

Table 6
Rotational and centrifugal distortion constants for the vibrational ground state of $H_2{}^{130}Te$ obtained by fitting the available experimental data with the Hamiltonian of Eq. (9)

A (MHz)	187.310510(43) [a]		
B (MHz)	182.757060(42)		
C (MHz)	91.011406(41)		
D_J (MHz)	11.1047(55)	H_J (kHz)	3.8958(699)
D_{JK} (MHz)	−40.1547(67)	H_{JK} (kHz)	−26.399(520)
D_K (MHz)	53.7048(50)	H_{KJ} (kHz)	28.610(708)
d_J (MHz)	5.16163(81)	H_K (kHz)	4.398(294)
d_K (MHz)	−4.7965(16)	h_J (kHz)	1.9117(514)
c_{22} (Hz)	132.4(21)	h_{JK} (kHz)	−7.327(218)
b_{03} (Hz)	−16.21(51)	h_K (kHz)	13.702(164)

[a] Quantities in parentheses are standard errors in units of the last digit given.

Table 7
Comparison of experimental and calculated vibrational energies E_{vib} and rotational constants A, B, and C for $H_2{}^{130}Te$ and $HD^{130}Te$ (in cm^{-1})

	(v_1, v_2, v_3)		E_{vib}	A	B	C
$H_2{}^{130}Te$	(0, 0, 0)	exp. [a]	0.0	6.2480	6.0961	3.0358
		calc.	0.0	6.1860	6.0182	3.0020
		exp. − calc.		0.0620	0.0779	0.0338
	(0, 1, 0)	exp. [b]	860.765	6.4296	6.2259	3.0056
		calc.	866.85	6.3559	6.1488	2.9721
		exp. − calc.	−6.09	0.0737	0.0771	0.0335
	(1, 1, 0)	exp. [c]	2911.416	6.3486	6.1364	2.9605
		calc.	2914.47	6.2770	6.0674	2.9297
		exp. − calc.	−3.05	0.0716	0.0690	0.0338
	(0, 1, 1)	exp. [c]	2915.97	6.3192	6.1646	2.9755
		calc.	2921.13	6.2493	6.0957	2.9434
		exp. − calc.	−5.16	0.0699	0.0689	0.0321
	(2, 0, 0)	exp. [d]	4062.889	6.0681	5.9419	2.9572
		calc.	4060.10	6.0032	5.8858	2.9008
		exp. − calc.	2.79	0.0649	0.0561	0.0564
	(1, 0, 1)	exp. [d]	4063.374	6.0622	5.9479	2.9594
		calc.	4061.00	5.9967	5.8925	2.9565
		exp. − calc.	2.37	0.0655	0.0554	0.0029
$HD^{130}Te$	(0, 0, 0)	exp. [c]	0.0	6.1685	3.1104	2.0422
		calc.	0.0	6.1005	3.0741	2.0191
		exp. − calc.		0.0680	0.0363	0.0231
	(2, 0, 0)	exp. [c]	4063.974	5.8377	3.1099	2.0068
		calc.	4061.63	5.7895	3.0716	1.9857
		exp. − calc.	2.34	0.0482	0.0383	0.0211

[a] Calculated from the parameter values in Table 6.
[b] From the analysis of the data by Hill et al. [19] carried out by Moncur et al. [23].
[c] Ref. [21]. [d] Ref. [23]. [e] Ref. [22].

where ω is the harmonic vibration wavenumber of the bending mode and A, B and C are the rotational constants given in cm^{-1}. For H_2Se and H_2S, we calculate J_{cr} to be 12 and 15, respectively [1–3]. For each of these two molecules, our MORBID calculations show that at $J \approx J_{cr}$, the energy separation between the two doublets at highest energy in the J multiplets of the vibrational ground state starts decreasing with increasing J. Hence we can say that for H_2Se and H_2S, the quantum mechanical MORBID calculations confirm the values of J_{cr} obtained from the semiclassical Eq. (10). However, as already discussed in Ref. [3], we calculate $J_{cr} = 8$ for the most abundant H_2Te isotopomer, $H_2{}^{130}Te$, using as input the rotational constants from Ref. [24] and the bending fundamental energy from Ref. [19], whereas it is seen from Fig. 2 that the energy difference between the two doublets at highest energy does not start decreasing with increasing J until $J \approx 12$, i.e., the same value as for H_2Se.

In Ref. [3], the low semiclassical J_{cr} value for $H_2{}^{130}Te$ led us to believe that for this molecule, the cluster states would be displaced dramatically towards lower J values relative to H_2Se, so that the transitions involving these states would be easily accessible to experimental investigation. The calculations of the present work provide substantial evidence that this is not the case. The clusters actually form at J-values comparable to those found for H_2Se. A possible reason for the failure of the semiclassical theory for H_2Te could be the simple fact that for $J < 10$ the behaviour of the H_2Te molecule is strictly quantum mechanical so that predictions based on semiclassical theory must necessarily fail.

Fig. 2 shows that in order to provide conclusive experimental evidence for the cluster formation in the vibrational ground state of H_2Te, it is desirable to observe transitions to the $J_{K_aK_c} = J_{J0}$, J_{J1}, J_{J-11}, and J_{J-12} states for J in the range from 20 to 25. Such transitions have been observed for H_2Se [10–12]. Obviously at a given temperature, the transitions to the cluster states are stronger in H_2Te than in H_2Se, since in the former, the lower states of these transitions are found at lower energies and are thus more heavily populated. In H_2Se the observation of the "cluster transitions" [10–12] was only made possible by heating the H_2Se sample to 90°C, however, at which temperature the H_2Te molecule will presumably decompose. Its spectrum must therefore be studied at lower temperatures for which the intensity advantage over H_2Se is likely to be lost. Hence we can conclude that the experimental observation of cluster states in H_2Te would seem to be at least as difficult as in H_2Se, so that experimental work on H_2Te will give us a "coverage" of the cluster states similar to that obtained for H_2Se [10–12,33], but not the significantly better coverage that we initially hoped for.

Acknowledgement

We are grateful to W. Thiel for supplying us with a copy of his effective core potential integral program and to P.R. Bunker, O.L. Polyansky, and B.P. Winnewisser for critically reading the manuscript and suggesting improvements. This work was supported by the Deutsche Forschungsgemeinschaft through Forschergruppe grant no. Bu 152/12-3 and by the Fonds der Chemischen Industrie. One of us (P.J.) acknowledges further support from the Dr. Otto Röhm Gedächtnisstiftung and from the Fritz Thyssen-Stiftung. The work of I.N.K. was supported by the Russian Fund for Fundamental Studies and the International Science Foundation (Reg. No. Ph3-1137). The present work has only been possible through the use of the Siemens/Nixdorf S100/10 supercomputer at the Justus Liebig University Giessen, which is made available to P.J. by the State of Hessen.

References

[1] P. Jensen and I.N. Kozin, J. Mol. Spectry. 160 (1993) 39.
[2] I.N. Kozin and P. Jensen, J. Mol. Spectry. 161 (1993) 186.
[3] I.N. Kozin and P. Jensen, J. Mol. Spectry. 163 (1994) 483.
[4] P. Jensen, J. Mol. Spectry. 128 (1988) 478.
[5] P. Jensen, J. Chem. Soc. Faraday Trans. II 84 (1988) 1315.
[6] P. Jensen, in: Methods in computational molecular physics, eds. S. Wilson and G.H.F. Diercksen (Plenum Press, New York, 1992).
[7] P. Jensen and P.R. Bunker, J. Mol. Spectry. 164 (1994) 315.
[8] P.R. Bunker, Molecular symmetry and spectroscopy (Academic Press, London, 1979).
[9] H.C. Longuet-Higgins, Mol. Phys. 6 (1963) 445.
[10] I.N. Kozin, S.P. Belov, O.L. Polyansky and M. Yu. Tretyakov, J. Mol. Spectry. 152 (1992) 13.
[11] I.N. Kozin, O.L. Polyansky, S.I. Pripolzin and V.L. Vaks, J. Mol. Spectry. 156 (1992) 504.
[12] I.N. Kozin, S. Klee, P. Jensen, O.L. Polyansky and I.M. Pavlichenkov, J. Mol. Spectry. 158 (1993) 409.
[13] B.I. Zhilinskii and I.M. Pavlichenkov, Opt. Spectry. (USSR) 64 (1988) 688.
[14] J. Makarewicz and J. Pyka, Mol. Phys. 68 (1989) 107.
[15] J. Makarewicz, Mol. Phys. 69 (1990) 903.
[16] J. Pyka, Mol. Phys. 70 (1990) 547.
[17] K.K. Lehmann, J. Chem. Phys. 95 (1991) 2361.
[18] K. Rossmann and J.W. Straley, J. Chem. Phys. 24 (1956) 1276.
[19] R.A. Hill, T.H. Edwards, K. Rossmann, K. Narahari Rao and H.H. Nielsen, J. Mol. Spectrosc. 14 (1964) 221.
[20] N.K. Moncur and T.H. Edwards, J. Chem. Phys. 51 (1969) 2638.
[21] N.K. Moncur, P.D. Willson and T.H. Edwards, J. Mol. Spectry. 52 (1974) 181.
[22] P.D. Willson, N.K. Moncur and T.H. Edwards, J. Mol. Spectry. 52 (1974) 196.
[23] N.K. Moncur, P.D. Willson and T.H. Edwards, J. Mol. Spectry. 52 (1974) 380.
[24] A.V. Burenin, A.F. Krupnov, S.V. Mart'yanov, A.A. Mel'nikov and L.I. Nikolayev, J. Mol. Spectry. 75 (1979) 333.
[25] K. Raghavachari, G.W. Trucks, J.A. Pople and M. Head-Gordon, Chem. Phys. Letters 157 (1989) 479.
[26] W.R. Wadt and J. Hay, J. Chem. Phys. 82 (1984) 284.
[27] T.H. Dunning, J. Chem. Phys. 90 (1989) 1007.
[28] S. Carter and N.C. Handy, J. Chem. Phys. 87 (1987) 4294.
[29] J.A. Fernley, S. Miller and J. Tennyson, J. Mol. Spectry. 150 (1991) 597.
[30] S.E. Choi and J.C. Light, J. Chem. Phys. 97 (1992) 7031.
[31] M.J. Bramley and T. Carrington Jr., J. Chem. Phys. 99 (1993) 8519.
[32] K. Sumathi and K. Balasubramanian, J. Chem. Phys. 92 (1990) 6604.
[33] J.-M. Flaud, C. Camy-Peyret, H. Bürger and H. Willner, J. Mol. Spectry. 161 (1993) 157.